International Journal of Internet, Broadcasting and Communication Vol.14 No.2 23-29 (2022)
http://dx.doi.org/10.7236/IJIBC.2022.14.2.23

IJIBC 22-2-4

An Analytical Expression for BER Performance of Intelligent Reflecting Surface Assisted NOMA

Kyuhyuk Chung

Professor, Department of Software Science, Dankook University, Korea
khchung@dankook.ac.kr

Abstract

To improve spectrum and energy efficiency in the fifth generation (5G) wireless channels, intelligent reflecting surface (IRS) transmissions have been envisioned, possibly towards the sixth generation (6G) networks. In this paper, we analyze the bit-error rate (BER) performance of intelligent reflecting surface (IRS) assisted non-orthogonal multiple access (NOMA) systems. First, we derive a closed-form expression of the BER in terms of Q functions. Then we analyze the BER improvement of the IRS NOMA system over the conventional NOMA system with respect to the power allocation. Furthermore, we also demonstrate numerically the BER improvement of the IRS NOMA network over the conventional NOMA network in respect of the number of reflecting devices.

Keywords: *Intelligent reflecting surface, 6G, NOMA, 5G, Power allocation.*

1. Introduction

Nowadays the most of mobile networks have been exploiting the fifth-generation (5G) communications [1]. Non-orthogonal multiple access (NOMA) has been one of the key technologies in 5G [2-4]. However, the spectral efficiency and power efficiency have been more important in the sixth-generation (6G) communications [5]. The intelligent reflecting surface (IRS) technology has been proposed to solve such demands [6-8]. Therefore, this low-cost antenna array can be applied to NOMA, i.e., IRS-NOMA, so that the connectivity and spectral efficiency would be improved by IRS-NOMA. The BER of the weaker channel gain user was analyzed for non-uniform source SSC NOMA [9]. A bit-to-symbol (BTS) mapping for NOMA with a non-uniform source and symmetric superposition coding (SSC) has been proposed [10]. In this paper, we investigate the bit-error rate (BER) performance of IRS assisted NOMA networks. First, we derive an analytical expression of the BER in terms of Q functions. Then we demonstrate numerically the BER improvement of the IRS NOMA system over the conventional NOMA system with respect to the power allocation. Furthermore, we also show numerically the BER improvement of the IRS NOMA network over the conventional NOMA network in respect of the number of reflecting devices.

The remainder of this paper is organized as follows. In Section 2, the system and channel model are described. An exact analytical expression for the average BER of IRS-NOMA over the Rayleigh fading

Manuscript Received: February. 6, 2022 / Revised: February. 10, 2022 / Accepted: February. 12, 2022
Corresponding Author: khchung@dankook.ac.kr
Tel: +82-32-8005-3237, Fax: +82-504-203-2043
Professor, Department of Software Science, Dankook University, Korea

channel of the direct link is derived in Section 3. The results of simulations are presented in Section 4. Finally, the conclusions are presented in Section 5.

The main contributions of this paper are summarized as follows:

- We derive an exact average closed-form expression for the BER of the IRS NOMA network in terms of Q functions.
- Then, we analyze the BER improvement of the IRS NOMA system over the conventional NOMA system with respect to the power allocation.
- Moreover, we also demonstrate numerically the BER improvement of the IRS NOMA network over the conventional NOMA network in respect of the number of reflecting devices.

2. System and Channel Model

We consider an IRS-NOMA transmission system from a single-antenna base station to two single-antenna users, namely a near user and a cell-edge user. Assume that there is a direct link between the base station and the cell-edge user, which is Rayleigh distributed, denoted by h_2 with the second moment $\Sigma_2 = \mathbb{E}\left[|h_2|^2\right]$. We assume that there is no direct link between the IRS and the near user. The base station broadcasts the superimposed signal $x = \sqrt{P\alpha}s_1 + \sqrt{P(1-\alpha)}s_2$, where the average total transmitted power is P, s_m is the signal with the average unit power for the mth user, $m = 1, 2$, and α is the power allocation coefficient. The signal r_2 received by the cell-edge user is expressed by

$$r_2 = |h|x + n_2, \tag{1}$$

where $h = h_2 + \mathrm{h}_{br}^T \Theta \mathrm{h}_{ru}$ and $n_2 \sim N(0, N_0/2)$ is additive white Gaussian noise (AWGN). For a given number N of reflecting devices, h_{br} denotes the $N \times 1$ deterministic flat-fading channel from the base station to the IRS and h_{ru} denotes the $N \times 1$ deterministic flat-fading channel from the IRS to the cell-edge user. The IRS is represented by the diagonal matrix $\Theta = \omega \,\mathrm{diag}\left(e^{j\theta_1}, \cdots, e^{j\theta_N}\right),$, where $\omega \in (0,1]$ is the fixed amplitude reflection coefficient and $\theta_1, \cdots, \theta_N$ are the phase-shift variables that can be optimized by the IRS. The IRS selects the phase-shifts to obtain the maximum channel gain, as follows:

$$|h|_{\max} = |h_2| + \underbrace{\omega \sum_{n=1}^{N} \left| \left(\mathrm{h}_{br}\right)_n \left(\mathrm{h}_{ru}\right)_n \right|}_{\xi} = |h_2| + \xi, \tag{2}$$

where $\xi = \omega \sum_{n=1}^{N} \left| \left(\mathrm{h}_{br}\right)_n \left(\mathrm{h}_{ru}\right)_n \right|$.

3. Derivation of Exact Average BER Expression for IRS-NOMA

We now derive an exact analytical expression for the average BER of IRS-NOMA over the Rayleigh fading channel of the direct link. Based on the previous work in [11], we start the following conditional BER given

the channel realization $|h_2|$:

$$P_{2||h_2|}^{(\text{IRS-NOMA})} = \frac{1}{2}Q\left(\frac{\left(|h_2|+\xi\right)\sqrt{P}\left(\sqrt{(1-\alpha)}-\sqrt{\alpha}\right)}{\sqrt{N_0/2}}\right)+\frac{1}{2}Q\left(\frac{\left(|h_2|+\xi\right)\sqrt{P}\left(\sqrt{(1-\alpha)}+\sqrt{\alpha}\right)}{\sqrt{N_0/2}}\right), \tag{3}$$

where $Q(y)=\int_y^{\infty}\frac{1}{\sqrt{2\pi}}e^{-\frac{(z)^2}{2}}dz$. Then we average $P_{2||h_2|}^{(\text{IRS-NOMA})}$ over the Rayleigh fading distribution,

$$P_2^{(\text{IRS-NOMA})} = \int_0^{\infty}\left(\frac{1}{2}Q\left(\frac{\left(|h_2|+\xi\right)\sqrt{P}\left(\sqrt{(1-\alpha)}-\sqrt{\alpha}\right)}{\sqrt{N_0/2}}\right)+\frac{1}{2}Q\left(\frac{\left(|h_2|+\xi\right)\sqrt{P}\left(\sqrt{(1-\alpha)}+\sqrt{\alpha}\right)}{\sqrt{N_0/2}}\right)\right)\cdot e^{-\frac{\left(|h_2|\right)^2}{\Sigma_2}}2\frac{\left(|h_2|\right)}{\Sigma_2}d|h_2|. \tag{4}$$

We integrate the first term T_1 in the integrand as follows:

$$\begin{aligned}
T_1 &= \int_0^{\infty}\frac{1}{2}Q\left(\frac{\left(|h_2|+\xi\right)\sqrt{P}\left(\sqrt{(1-\alpha)}-\sqrt{\alpha}\right)}{\sqrt{N_0/2}}\right)e^{-\frac{\left(|h_2|\right)^2}{\Sigma_2}}2\frac{\left(|h_2|\right)}{\Sigma_2}d|h_2| \\
&= \int_0^{\infty}\frac{1}{2}Q\left(\sqrt{2\gamma_{b,\text{norm}}\Sigma_2\left(g_2+\frac{\xi}{\sqrt{\Sigma_2}}\right)^2}\right)e^{-\frac{\left(\sqrt{\Sigma_2}g_2\right)^2}{\Sigma_2}}2\frac{\left(\sqrt{\Sigma_2}g_2\right)}{\Sigma_2}\left(\sqrt{\Sigma_2}dg_2\right) \\
&= \int_0^{\infty}\frac{1}{2}Q\left(\sqrt{2\gamma_b\left(g_2+\xi_{,\text{norm}}\right)^2}\right)e^{-\left(|g_2|\right)^2}2g_2dg_2 = \int_{\xi_{,\text{norm}}}^{\infty}\frac{1}{2}Q\left(\sqrt{2\gamma_b x^2}\right)e^{-\left(x-\xi_{,\text{norm}}\right)^2}2\left(x-\xi_{,\text{norm}}\right)dx,
\end{aligned} \tag{5}$$

where we define the SNR as $\gamma_{b,\text{norm}}=\frac{P\left(\sqrt{(1-\alpha)}-\sqrt{\alpha}\right)^2}{N_0}$ with $\gamma_b=\Sigma_2\gamma_{b,\text{norm}}$, $\xi_{\text{norm}}=\frac{\xi}{\sqrt{\Sigma_2}}$, and we change the variables $\sqrt{\Sigma_2}g_2=|h_2|$ and $x=|g_2|+\xi_{,\text{norm}}$. Now we perform the integration by parts

$$\begin{aligned}
T_1 &= \frac{1}{2}\left[\left(-e^{-\left(x-\xi_{,\text{norm}}\right)^2}\right)\cdot Q\left(\sqrt{2\gamma_b x^2}\right)\right]_{x=\xi_{\text{norm}}}^{\infty}-\frac{1}{2}\int_{\xi_{\text{norm}}}^{\infty}\frac{d}{dx}\left(\int_{\sqrt{2\gamma_b x^2}}^{\infty}\frac{1}{\sqrt{2\pi}}e^{-\frac{(z)^2}{2}}dz\right)\cdot\left(-e^{-\left(x-\xi_{\text{norm}}\right)^2}\right)dx \\
&= \frac{1}{2}\left[0-(-1)\cdot Q\left(\sqrt{2\gamma_b\xi_{\text{norm}}^2}\right)\right]-\frac{1}{2}\int_{\xi_{\text{norm}}}^{\infty}\left(0-\frac{1}{\sqrt{2\pi}}e^{-\gamma_b x^2}\cdot\left(\sqrt{2\gamma_b}\right)\right)\cdot\left(-e^{-\left(x-\xi_{\text{norm}}\right)^2}\right)dx \\
&= \frac{1}{2}Q\left(\sqrt{2\gamma_b\xi_{\text{norm}}^2}\right)-\frac{1}{2}\sqrt{\gamma_b}\frac{1}{\sqrt{\pi}}e^{-\left(\frac{\gamma_b}{(1+\gamma_b)}\right)\xi_{\text{norm}}^2}\int_{\xi_{\text{norm}}}^{\infty}e^{-(1+\gamma_b)\left(x-\frac{\xi_{\text{norm}}}{(1+\gamma_b)}\right)^2}dx.
\end{aligned} \tag{6}$$

By changing the variable $x-\frac{\xi_{\text{norm}}}{(1+\gamma_b)}=y$, we have

$$T_1 = \frac{1}{2}Q\left(\sqrt{2\gamma_b \xi_{\text{norm}}^2}\right) - \frac{1}{2}\sqrt{\gamma_b}\,\frac{1}{\sqrt{\pi}} e^{-\left(\frac{\gamma_b}{(1+\gamma_b)}\right)\xi_{\text{norm}}^2} \int_{\xi_{\text{norm}} - \frac{\xi_{\text{norm}}}{(1+\gamma_b)}}^{\infty} e^{-\frac{\left(\sqrt{2(1+\gamma_b)}y\right)^2}{2}} dy. \tag{7}$$

Again by changing the variable $\sqrt{2(1+\gamma_b)}y = x$, we have

$$\begin{aligned} T_1 &= \frac{1}{2}Q\left(\sqrt{2\gamma_b \xi_{\text{norm}}^2}\right) - \frac{1}{2}\sqrt{\gamma_b}\,\frac{1}{\sqrt{\pi}} e^{-\left(\frac{\gamma_b}{(1+\gamma_b)}\right)\xi_{\text{norm}}^2} \int_{\sqrt{2(1+\gamma_b)}\xi_{\text{norm}}\left(1-\frac{1}{(1+\gamma_b)}\right)}^{\infty} e^{-\frac{(x)^2}{2}} \frac{1}{\sqrt{2(1+\gamma_b)}} dx \\ &= \frac{1}{2}Q\left(\sqrt{2\gamma_b \xi_{\text{norm}}^2}\right) - \frac{1}{2}Q\left(\sqrt{2(1+\gamma_b)\xi_{\text{norm}}^2\left(\frac{\gamma_b}{1+\gamma_b}\right)}\right) e^{-\left(\frac{\gamma_b}{(1+\gamma_b)}\right)\xi_{\text{norm}}^2} \sqrt{\frac{\gamma_b}{1+\gamma_b}}. \end{aligned} \tag{8}$$

Similarly, by integrating the second term T_2 in the integrand in (4), finally $P_2^{(\text{IRS-NOMA})}$ is expressed as

$$\begin{aligned} P_2^{(\text{IRS-NOMA})} &= \frac{1}{2}Q\left(\sqrt{2\gamma_b \xi_{\text{norm}}^2}\right) - \frac{1}{2}Q\left(\sqrt{2(1+\gamma_b)\xi_{\text{norm}}^2\left(\frac{\gamma_b}{1+\gamma_b}\right)}\right) e^{-\left(\frac{\gamma_b}{(1+\gamma_b)}\right)\xi_{\text{norm}}^2} \sqrt{\frac{\gamma_b}{1+\gamma_b}} \\ &+ \frac{1}{2}Q\left(\sqrt{2\gamma_c \xi_{\text{norm}}^2}\right) - \frac{1}{2}Q\left(\sqrt{2(1+\gamma_c)\xi_{\text{norm}}^2\left(\frac{\gamma_c}{1+\gamma_c}\right)}\right) e^{-\left(\frac{\gamma_c}{1+\gamma_c}\right)\xi_{\text{norm}}^2} \sqrt{\frac{\gamma_c}{1+\gamma_c}}, \end{aligned} \tag{9}$$

where $\gamma_c = \Sigma_2 P\left(\sqrt{(1-\alpha)} + \sqrt{\alpha}\right)^2 / N_0$. Although it is difficult to obtain a generalized equation currently, the extension to a network for more than two users can be achieved by algebraic manipulations.

4. Numerical Results and Discussions

In this section, numerical results are presented to validate the theoretical results; for this, $\omega = 1$, $\Sigma_2 = 0.2$, $\left(\mathrm{h}_{br}\right)_n = 0.01$ and $\left(\mathrm{h}_{ru}\right)_n = 0.01$. In Figure 1, first, we depict the normalized ξ, i.e. ξ_{norm}, versus the number of devices, to analyze numerically the impact of the number of devices on the normalized ξ. Remark that we consider the exact BER for deterministic flat-fading channels h_{br} and h_{ru}, so that we present numerical results only for large-scale fading channels h_{br} and h_{ru}, with small-scale fading h_2.

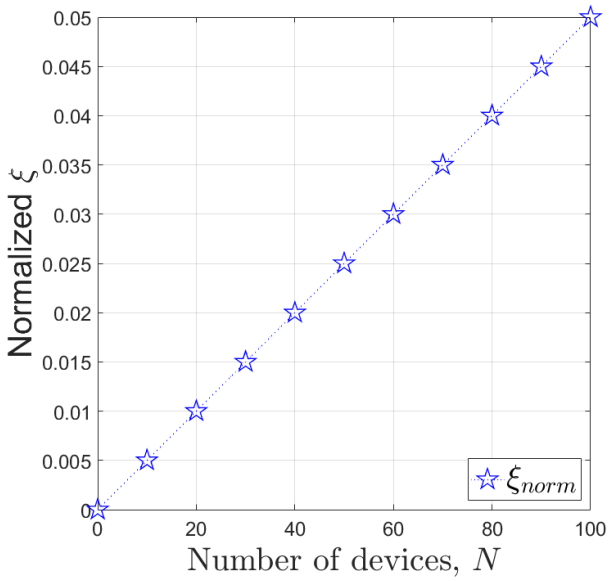

Figure 1. Normalized ξ versus the number of reflecting devices

As shown in Figure 1, we observe the intuitive result that the normalized ξ increases monotonically with the number of reflecting elements *N*; hence, when we calculate the BER, we choose the number of devices $N = 100$.

Second, to investigate the BER improvement, we depict the BERs versus the power allocation, $0 \le \alpha \le 0.5$ (dB), with $N = 100$, in Figure 2.

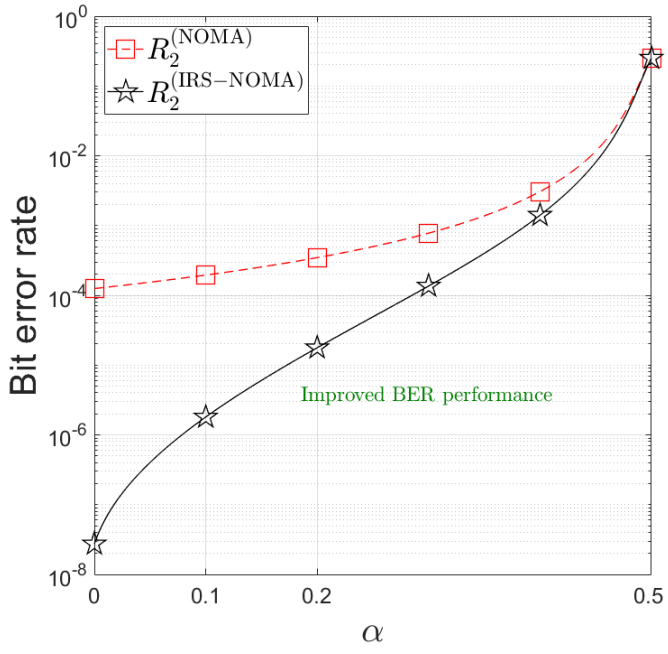

Figure 2. Comparison of BERs of IRS-NOMA and NOMA systems, ($0 \le \alpha \le 0.5$)

As shown in Figure 2, the BER of the IRS-NOMA system improves over the entire power allocation range, i.e., $0 \le \alpha \le 0.5$, compared to that of the NOMA system. Note that in NOMA, the channels are shared by users, so that the user-fairness should be established among users. In this case, the power allocation coefficient should be at least less than 0.5.

Third, to investigate the BER improvement in term of reflecting elements N, we depict the BERs versus N, with $\alpha = 0.1$, in Figure 3.

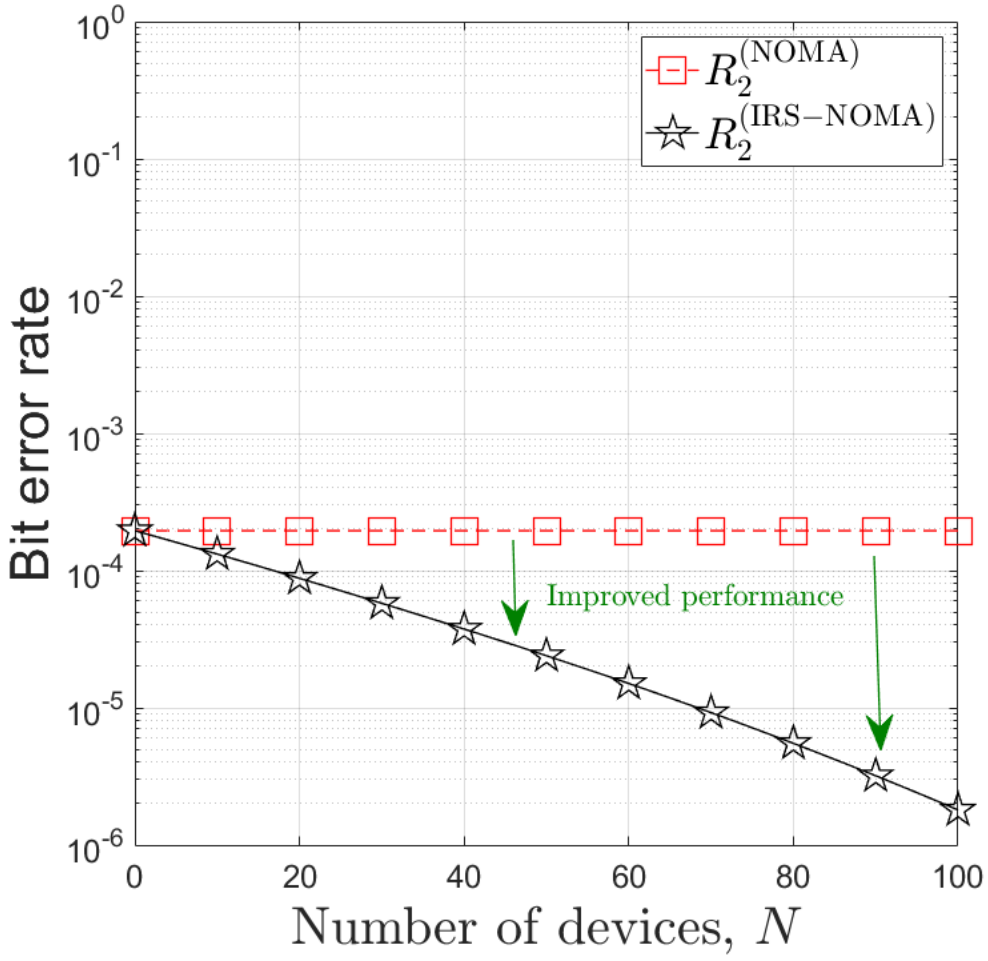

Figure 3. Comparison of BERs of IRS-NOMA and NOMA systems, ($0 \le N \le 100$)

As shown in Figure 3, we observe that the BER improvement increases significantly with the number of reflecting elements N.

5. Conclusion

In the paper, we analyzed the BER performance of IRS assisted NOMA systems. First, we derived an exact closed-form expression for the BER in terms of Q functions. Then we demonstrated numerically the BER improvement of the IRS NOMA system over the conventional NOMA system with respect to the whole power allocation range less than 0.5. Furthermore, we also showed numerically the BER improvement of the IRS

NOMA network over the conventional NOMA network in respect of the number of reflecting devices.

As a result, the IRS transmission could be a promising technology for 5G NOMA networks possibly towards 6G mobile communications.

References

[1] L. Chettri and R. Bera, "A comprehensive survey on internet of things (IoT) toward 5G wireless systems," *IEEE Internet of Things Journal*, vol. 7, no. 1, pp. 16–32, Jan. 2020. DOI: https://doi.org/10.1109/JIOT.2019.2948888

[2] Y. Saito, Y. Kishiyama, A. Benjebbour, T. Nakamura, A. Li, and K. Higuchi, "Non-orthogonal multiple access (NOMA) for cellular future radio access," in *Proc. IEEE 77th Vehicular Technology Conference (VTC Spring)*, pp. 1–5, 2013. DOI: https://doi.org/10.1109/VTCSpring.2013.6692652

[3] Z. Ding, P. Fan, and H. V. Poor, "Impact of user pairing on 5G nonorthogonal multiple-access downlink transmissions," *IEEE Trans. Veh. Technol.*, vol. 65, no. 8, pp. 6010–6023, Aug. 2016. DOI: https://doi.org/10.1109/TVT.2015.2480766

[4] Z. Ding, X. Lei, G. K. Karagiannidis, R. Schober, J. Yuan, and V. Bhargava, "A survey on non-orthogonal multiple access for 5G networks: Research challenges and future trends," *IEEE J. Sel. Areas Commun.*, vol. 35, no. 10, pp. 2181–2195, Oct. 2017. DOI: https://doi.org/10.1109/JSAC.2017.2725519

[5] E. C. Strinati *et al*., "6G: The next frontier: From holographic messaging to artificial intelligence using subterahertz and visible light communication," *IEEE Veh. Technol. Mag*., vol. 14, no. 3, pp. 42–50, Sept. 2019. DOI: https://doi.org/10.1109/MVT.2019.2921162

[6] Q. Wu and R. Zhang, "Intelligent reflecting surface enhanced wireless network via joint active and passive beamforming," *IEEE Trans. Wireless Commun*., vol. 18, no. 11, pp. 5394–5409, Nov. 2019.

[7] C. Huang, A. Zappone, G. C. Alexandropoulos, M. Debbah, and C. Yuen, "Reconfigurable intelligent surfaces for energy efficiency in wireless communication," *IEEE Trans. Wireless Commun*., vol. 18, no. 8, pp. 4157–4170, Aug. 2019.

[8] Q. Wu and R. Zhang, "Towards smart and reconfigurable environment: Intelligent reflecting surface aided wireless network," *IEEE Commun. Mag*., vol. 58, no. 1, pp. 106–112, Jan. 2020.

[9] K. Chung, "Impacts of Non-Uniform Source on BER for SSC NOMA (Part II): Improved BER Performance Analysis," *International Journal of Internet, Broadcasting and Communication (IJIBC)*, vol. 13, no. 4, pp. 48–54, Nov. 2021. DOI: http://dx.doi.org/10.7236/IJIBC.2021.13.4.48

[10] K. Chung, "BTS Based Improved BER for Stronger Channel User in Non-Uniform Source SSC NOMA," *International Journal of Internet, Broadcasting and Communication (IJIBC)*, vol. 14, no. 1, pp. 78–84, Feb. 2022. DOI: http://dx.doi.org/10.7236/IJIBC.2022.14.1.78

[11] K. Chung, "Performance Analysis for Weaker Channel User in Non-Uniform Source SSC NOMA with Novel BTS," *International Journal of Advanced Smart Convergence (IJASC)*, vol. 11, no. 1, pp. 36-41, Mar. 2022. DOI: http://dx.doi.org/10.7236/IJASC.2022.11.1.36